

# Effect of atomic-scale randomness on the optical polarization of semiconductor quantum dots

Vladan Mlinar and Alex Zunger\*

National Renewable Energy Laboratory, Golden, Colorado 80401, USA

(Received 9 January 2009; published 13 March 2009)

Alloy systems such as  $\text{Ga}_{1-x}\text{In}_x\text{As}$  consist of different random assignments  $\sigma$  of the Ga and In atoms onto the cation sublattice; each configuration  $\sigma$  having, in principle, distinct physical properties. In infinitely large bulk samples different  $\sigma$ 's get self-averaged. However, in finite quantum dots (QDs) ( $\leq 10^5$  atoms), self-averaging of such configuration  $\sigma$  may not be complete, so single-dot spectroscopy might observe atomic-scale alloy randomness effects. We examine theoretically the effect of such atomic-scale alloy randomness on the fine structure-splitting (FSS) of the multiexciton observed via the polarization anisotropy of its components. We find that (i) The FSS of the neutral monoexciton  $X^0$  changes by more than a factor of 7 with  $\sigma$ . Thus, dots provide clear evidence for the effect of the atomic-scale alloy randomness on the optical properties. (ii) For multiexcitons, the effect of alloy randomness can be so large that the polarization of given emission lines in samples that differ only in random realizations can be dramatically different, so it cannot be said that given transitions have fixed polarization. (iii) Polarization is affected both by atomic-scale randomness and by possible geometric elongation of the QD in one direction. Because of different random realizations, even 50% QD base elongation in [100] direction gives the same polarization as in a geometrically symmetric dot. Thus, measured polarization cannot be used to determine QD elongation.

DOI: [10.1103/PhysRevB.79.115416](https://doi.org/10.1103/PhysRevB.79.115416)

PACS number(s): 78.67.Hc, 71.35.Ji, 73.21.La

## I. INTRODUCTION

Pure material components A and B are often alloyed to yield  $\text{A}_{1-x}\text{B}_x$  (where  $x$  is the composition) to achieve target physical properties that are intermediate between those of the end-point components.<sup>1,2</sup> In general, the  $\text{A}_{1-x}\text{B}_x$  random alloy can be thought of as an average over many independent random realizations (RRs), each being a particular random assignment of atoms A and B to each of the  $N$  lattice sites.<sup>2,3</sup> In principle, each such random realization has distinct physical properties (e.g., band gap, level splittings, etc.). In bulk solids with their large numbers of lattice sites  $N$  ( $\sim$ Avogadro's number), the measured physical property, representing average over all RRs, often does not resolve the properties of individual RRs.<sup>2</sup> The emergence of single-dot spectroscopy<sup>4-8</sup> on alloy quantum dots (QDs) made of a finite number of atoms ( $N \leq 10^5$ ) has opened the possibility of observing the effects of individual random realizations. In this paper we focus on the influence of RRs on the emission from monoexciton ( $X^0$ ) in a  $\text{Ga}_{1-x}\text{In}_x\text{As}/\text{GaAs}$  QD. A particularly convenient feature for studying this is the fine-structure splitting (FSS) of the neutral exciton  $X^0$  [Fig. 1(a)], yielding two optically active transitions [2 and 3 in Fig. 1(a)] split typically by a few tens of  $\mu\text{eV}$ , and each linearly polarized along two orthogonal axes of the QD.<sup>9,10</sup> The difference in intensity between these two transitions is the measured polarization anisotropy. The magnitude of the FSS and the polarization directions of two transitions have recently attracted significant attention because of potential application of QDs as single-photon sources.<sup>11</sup> The requirement for a QD in such applications is that the emitted photons would be distinguishable only by polarization, so the FSS needs to ideally vanish. Indeed, seeking dots with small FSS is often done via "cherry picking" of individual dots out of a large ensemble grown on a wafer.<sup>8</sup> Recent polarization-resolved photoluminescence (PL) measurements on several different

QD samples have revealed a huge fluctuations of polarization anisotropy from one dot to another both in sign and magnitude.<sup>12-14</sup> Such polarization anisotropy is commonly believed<sup>10,12,15-17</sup> to result only from a geometric anisotropy of the dot, e.g., if the base of the dot is not circular (axis  $L1=L2$ ) but is instead elliptical ( $L1 \neq L2$ ). In fact, the polarization ratio of  $X^0$  has been recently proposed<sup>15</sup> as a *measure* of geometric asymmetry  $L1/L2$ . However, atomistic theory<sup>9</sup> reveals that FSS is nonzero even for geometrically symmetric ( $L1=L2$ ) dots (because the underlying lattice symmetry allows it). Could it be that the polarization anisotropy reflects also different random realizations at fixed  $L1, L2$  (and thus cannot be used to determine  $L1/L2$ )? In this paper we will show that, because of different random realizations, even 50% QD base elongation ( $L1/L2=1.5$ ) in [100] direction gives the same polarization as in a geometrically symmetric dot ( $L1/L2=1$ ). Furthermore, it was suggested by Poem *et al.*<sup>6</sup> that different multiexciton emission lines (not just  $X^0$ ) in alloy dots have well defined polarizations. Can we indeed talk about characteristic polarization of given exciton states, or does it depend on the (experimentally uncontrollable) RRs?

Theoretical investigation of the effect of atomic-scale alloy randomness on the electronic properties of an alloy QD requires an atomistic representation of alloy, where each of the  $N$  atoms in the alloy has its own, distinct local environment for each random realization (e.g., each As is coordinated by  $n$  In and  $4-n$  Ga atoms, where  $0 \leq n \leq 4$ , varies at different As sites). Clearly, such effects cannot be treated by continuumlike alloy theories, given that they represent alloy physics by a single (averaged) type of local environment, using parameters that are only composition dependent, but configuration independent.<sup>16</sup>

Because of the finite and small size of QDs, alloy randomness effects do not self-average, as they do in large samples. We show that such dots thus provide clear evidence for the effect of atomic-scale alloy randomness on the optical

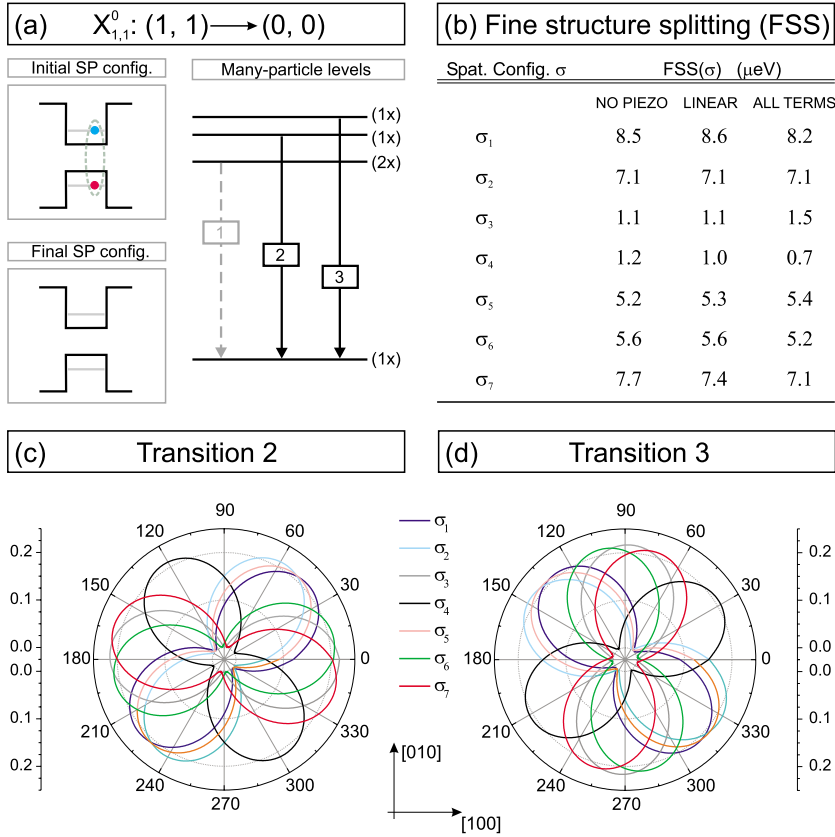


FIG. 1. (Color online) Fine structure splittings of monoexciton of a geometrically symmetric lens shaped  $\text{Ga}_{0.4}\text{In}_{0.6}\text{As}/\text{GaAs}$  QD with diameter 25 nm and height 2 nm: (a) shows schematic plot of FSS, on the left we show the dominant initial and final single-particle configurations and on the right the energy levels that correspond to many-body state. (b) shows our calculated FSS (in  $\mu\text{eV}$ ) as it varies with different random realizations  $\sigma$  in the absence of piezo field (No Piezo) and with piezoelectric field that includes only linear term<sup>22,23</sup> (Linear) and both linear and non-linear terms<sup>24,25</sup> (all terms). (c) and (d) show polar plots of the polarization directions for transition 2 and transition 3, respectively, for seven different values of  $\sigma$ .

properties. Using an atomistic description we find that (i) FSS is very sensitive on different RRs as it varies more than by a factor of 7 with RR. (ii) The polarization anisotropy of  $X^0$  transitions is caused both by different atomic-scale randomness and by possible QD elongation. Thus, measuring the polarization anisotropy cannot be used as a measure of geometrical anisotropy alone, and (iii) the polarization directions of multiexcitonic transitions depend heavily of random realization, so different multiexciton emission lines do not have fixed, characteristic polarization directions.

## II. METHOD

Our model QD is defined through its geometry (shape, base length, and height) and composition  $[X(\text{In})]$ . The  $N_{\text{cat}}$  cation sites of the  $\text{Ga}_{1-x}\text{In}_x\text{As}$  alloy are randomly populated by In or Ga atoms so that overall composition is  $x=X(\text{In})$ . Then, the atomic positions  $\{\mathbf{R}_{i,\alpha}\}$  are relaxed via valence force field method.<sup>18</sup> Screened-strain-dependent atomic pseudopotential  $v_\alpha(\mathbf{r})$  (fitted to bulk properties of InAs and GaAs, including bulk band structures, experimental deformation potentials, and effective masses) are placed on each relaxed site of atom of type  $\alpha$ . The total pseudopotential of the system  $V(\mathbf{r})=V_{\text{so}}+\sum_{i,\alpha}v_\alpha(\mathbf{r}-\mathbf{R}_{i,\alpha})$  is constructed by superposing the nonlocal spin-orbit interaction,  $V_{\text{so}}$ , to this local screened pseudopotential,  $v_\alpha(\mathbf{r})$ , of all atoms. The Hamiltonian  $-1/2\nabla^2+V(\mathbf{r})$  is diagonalized in a basis  $\{\phi_{n,\epsilon,\lambda}(\mathbf{k})\}$  of Bloch bands, of band index  $n$  and wave vector  $\mathbf{k}$  for material  $\lambda$  (InAs, GaAs),<sup>19</sup> yielding as solutions single-particle electron  $\{e_0, e_1, e_2, \dots\}$  and hole  $\{h_0, h_1, h_2, \dots\}$  states. These are

then used as a basis for the configuration-interaction method to access multiexcitonic states.<sup>20</sup> The emission intensity spectrum of a (multi)exciton,  $\chi$ , for polarization vector  $\hat{e}$  of the electromagnetic field, is given by<sup>21</sup>

$$I^{(e)}(\omega, T, \chi) = \sum_{i,f} |M_{if}^{(e)}(\chi)|^2 P_i(T, \chi) \delta[\omega - \omega_{if}(\chi)], \quad (1)$$

where  $M_{if}^{(e)}(\chi)$  is the transition dipole matrix element,  $P_i(T, \chi)$  is occupation (Boltzmann) probability of the initial state at temperature  $T$ , and  $\omega_{if}(\chi)$  is the transition energy. We use first a geometrically symmetric ( $L_1=L_2$ ) lens-shaped  $\text{Ga}_{0.4}\text{In}_{0.6}\text{As}$  QD with diameter  $L_1=L_2=25$  nm, and height  $h=2$  nm, sitting on 2 ML wetting layer (WL), with monoexciton energy  $E_X^0=1.308$  eV. We repeat the above calculation for ten independent random realizations, at the same composition. Our model QD is chosen such to represent QDs on which single-dot spectroscopy measurements were performed (with measured monoexciton energies  $\sim 1.3$  eV).<sup>6,12,27</sup>

## III. POLARIZATION DIRECTIONS AND OPTICAL ANISOTROPY FOR NEUTRAL EXCITON

### A. FSS and polarization directions of a geometrically symmetric dot

Figure 1(a) shows a schematic plot of FSS due to electron-hole recombination in a neutral exciton. The initial state has one electron (blue/dark gray) in the conduction band and one hole (red/gray) in the valence band. Including spin, each of these states has multiplicity 2, so the electron-

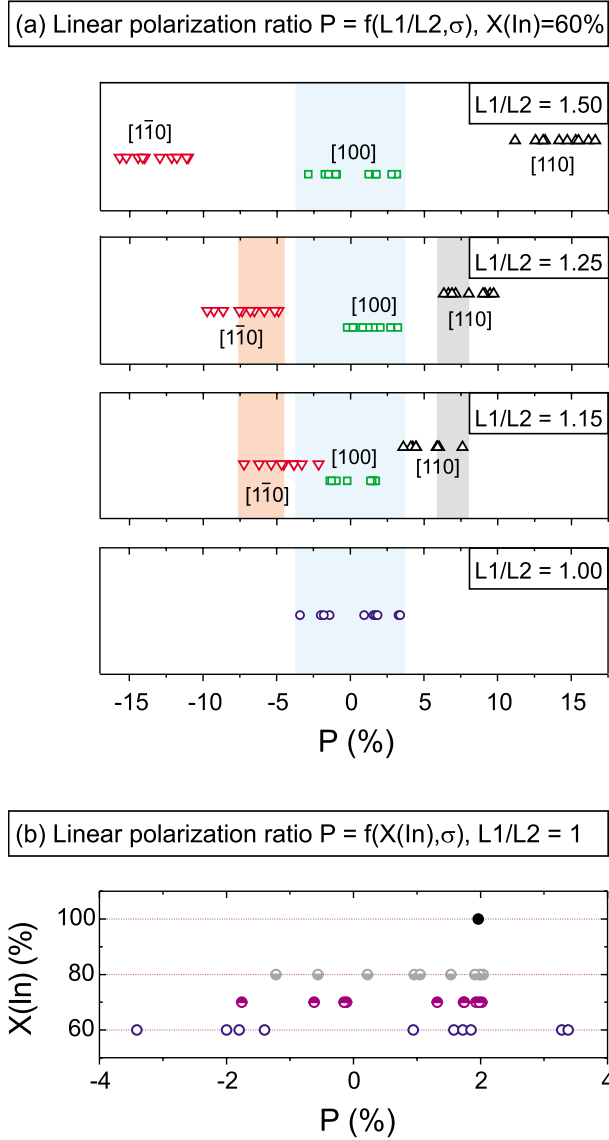


FIG. 2. (Color online) Variation in the linear polarization ratio ( $P$ ) with random realization  $\sigma$  for (a) circular-base QD, where axis  $L1=L2$  (blue/dark gray open circles), dot elongated ( $L1 \neq L2$ ) in  $[100]$  direction (green/light gray squares),  $[1\bar{1}0]$  direction (inverted red/gray triangles), and in  $[110]$  direction (black triangles). (b) Different indium concentrations [ $X(\text{In})=60, 70, 80,$  and  $100\%$ ].

hole exciton has a multiplicity  $2 \times 2 = 4$ . Electron-hole exchange interaction then causes splitting into  $2+1+1$ , where the lowest state ( $2 \times$ ) is dark [denoted as transition 1 in Fig. 1(a)] and transitions 2 and 3 are optically active. Figure 1(b) shows the calculated variation of FSS with different random realizations. Interestingly, while FSS exhibits significant dependence on the RR (from 1.1 to  $8.5 \mu\text{eV}$ ), it shows almost no sensitivity to the piezoelectric field, irrespective of piezoelectricity was included via linear term only,<sup>22,23</sup> or both linear and nonlinear terms.<sup>24,25</sup> The polar plots in Figs. 1(c) and 1(d) show the polarization directions of transition 2 and transition 3 of Fig. 1(a) as they vary with the RR. Remarkably, the polarization of transitions 2 and 3 can even change directions (e.g., compare polarization directions for random configurations  $\sigma_1, \sigma_3,$  and  $\sigma_4$ ). However, transitions 2 and 3

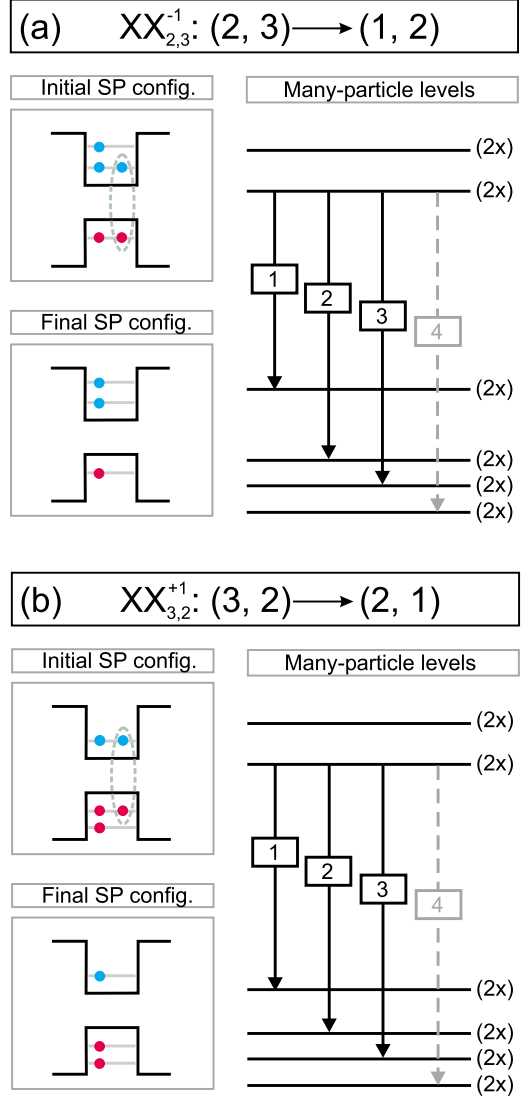


FIG. 3. (Color online) Schematic plot of initial and final single-particle (SP) and the initial and final many-particle levels for multiexcitonic transitions (a) ( $N_h=2, N_e=3$ )  $\rightarrow (1, 2)$  and (b) ( $N_h=3, N_e=2$ )  $\rightarrow (2, 1)$ .

are *always* aligned along orthogonal axes. Note that the variation with the RR of the polarization directions of transitions 2 and 3 and their FSS are correlated. For example, for  $\text{RR}=\sigma_1$ , transition 2 [blue curve in Fig. 1(c)] is oriented approximately along  $[110]$  direction (and transition 3, consequently, along  $[1\bar{1}0]$ ), and  $\text{FSS}(\sigma_1)=8.5 \mu\text{eV}$ , but when  $\text{RR}=\sigma_3$ , transition 2 [gray curve in Fig. 1(c)] is oriented approximately along  $[100]$  direction (and transition 3 along the  $[010]$ ), and  $\text{FSS}(\sigma_3)=1.1 \mu\text{eV}$ .

Note that, whereas the influence of QD base elongation and/or piezoelectricity on the fine structure splitting can be quantified deterministically (using e.g., k.p,<sup>10</sup> tight-binding,<sup>15</sup> or empirical pseudopotential methods<sup>9,23</sup>), the effect of the atomic-scale alloy randomness is not deterministically controlled. Thus, even if structurally identical, two dots are likely to have different RRs, and consequently different FSS. This sets up the upper limit for structural uniformity of two alloyed dots and their applications as single-photon sources.

TABLE I. Polarization directions of optically active transitions of multiexcitons, defined by angle  $\theta_p$  (in deg.) relative to  $[100]$  direction (see Fig. 3 for the case of  $X^{-2}$ ), where  $\sigma_i$  denotes a particular random realization. When a transition of ME has two distinct polarization directions, we give angles for both of those directions.

(Multi) exciton	Transition 1			Transition 2			Transition 3			Transition 4			Transition 5			Transition 6			
	$\sigma_1$	$\sigma_2$	$\sigma_3$	$\sigma_1$	$\sigma_2$	$\sigma_3$	$\sigma_1$	$\sigma_2$	$\sigma_3$	$\sigma_1$	$\sigma_2$	$\sigma_3$	$\sigma_1$	$\sigma_2$	$\sigma_3$	$\sigma_1$	$\sigma_2$	$\sigma_3$	
$X^0$		Dark		45	0	126	135	90	36										
$XX^0$	135	90	36	45	0	126		Dark											
$X^{-2}$		Dark		135	45	126	45	135	36	45;135	135;45	45;135	45	135	36	135	45	126	
$XX^{-1}$	90;9	9;99	90;0	171;54	36;135	171;108	45;135	90;45	27;72		Dark								
$XX^{+1}$	99;9	99;9	45;135	144;54	9;99	9;99	171;81	108;189	144;54		Dark								

### B. Linear polarization ratio: Atomic-scale alloy randomness vs geometric base anisotropy

The linear polarization ratio  $P$  is a measure<sup>9,12</sup> of the in-plane polarization anisotropy, and is defined as  $P=(I_x - I_y)/(I_x + I_y)$ , where  $I_x$  and  $I_y$  are intensities, given by Eq. (1), along  $[110]$  and  $[1\bar{1}0]$  directions, respectively. Since the RR influences the polarization directions of an alloy QD, it can be expected that  $P$  could vary with different RRs. This is examined in Figs. 2(a) and 2(b) by blue circles for our *geometrically symmetric*  $L1/L2=1$  QD having a circular base. We find that  $P(\sigma)$  adopts both positive and negative values even for the circular-base dot [light blue region in Fig. 2(a)], the controlling factor being different RR. If we increase indium concentration from  $X(\text{In})=60\%$  to  $X(\text{In})=70, 80, 100\%$ , the effect of atomic-scale alloy randomness on the polarization decreases, and  $P(\sigma)$  converges to a single value for  $X(\text{In})=100\%$ , as illustrated in Fig. 2(b).

We next elongate the dot base from  $L1=L2=1$  to  $L1/L2=1.15, 1.25, 1.5$  in  $[100], [110]$ , and  $[1\bar{1}0]$  directions, keeping the same volume as their circularly-based counterpart, and generate ten RRs for each base elongation. Figure 2(a) shows variation of  $P$  with base elongation and RRs. We see that:

(i) The variation in sign and magnitude of  $P(\sigma)$  of different RRs for the geometrically elongated dot in  $[100]$  direction [green squares in Fig. 2(a)] is well within the range of  $P(\sigma)$  for symmetric, circular-base QDs.

(ii)  $P(\sigma)$  is always negative for dots elongated in the  $[1\bar{1}0]$  direction [red inverted triangles in Fig. 2(a)], and positive for  $[110]$  [black triangles in Fig. 2(a)]. Interestingly, there is an overlap between  $P(\sigma)$  of circular-base dot and  $P(\sigma)$  of dot elongated by  $L1/L2 \leq 1.15$  either in  $[110]$  or  $[1\bar{1}0]$  direction. For example,  $P=-2.36$  for  $L1/L2=1.15$  in  $[1\bar{1}0]$  direction which is within the range of  $P(L1/L2=1, \sigma)$ . Also, there is an overlap between  $P(\sigma)$  of the dot with the base elongated by  $L1/L2=1.15$  and  $P(\sigma)$  for  $L1/L2=1.25$  [see light-red region for the dot base elongated in  $[1\bar{1}0]$  direction and gray region for  $[110]$  direction, in Fig. 2(a)]. This means that the effect of atomic-scale randomness on the range of polarization anisotropy can overwhelm the effect of geometric base elongation.

### C. Comparison with other calculations

Recent effective bond orbital model (EBOM) calculations<sup>15</sup> illustrated variation of  $P$  with different RRs

for a single, fixed QD geometry (lens with height  $h=5.1$  nm and elongation of 50% in  $[1\bar{1}0]$  direction) and fixed composition [ $X(\text{In})=80\%$ ]. The authors in Ref. 15 found that for their particular dot,  $P$  varies from 18% to 23%, i.e., by 5%, with different random realizations, concluding that “random intermixing effect... does not affect much on the optical anisotropy.” They further conclude that “the polarization property is shown to be insensitive to the random intermixing effect which makes it an appropriate tool for characterizing structure for quantum dots.” Although, we find similar range of polarizations,  $P$  varies from  $(-15)$  to  $(-11)\%$  [see inverted red triangles in top panel of Fig. 2(a)] for our model dot [ $h=2$  nm,  $X(\text{In})=60\%$ ] elongated by 50% in  $[1\bar{1}0]$  direction. Sheng and Xu<sup>15</sup> explore profiles over the dot and we explore atom by atom substitution. Furthermore, our broader study leads to very different conclusions than Ref. 15. Indeed, by considering different directions and degrees of elongation [Fig. 2(a)] and several indium compositions [Fig. 2(b)], we find that  $P$  cannot be used as a tool for structural characterization because (i) *measuring*  $P$  cannot tell the geometrical anisotropy: Fig. 2(a) shows QD base elongation of up to 50% in  $[100]$  direction have the same range of  $P$  as the circular-base model dot, or up to 15% in  $[110]$  (or  $[1\bar{1}0]$ ) direction; (ii) *measuring*  $P$  does not tell the composition, as Fig. 2(b) shows the dot composition  $X(\text{In})=60\%, X(\text{In})=70\%$ , and  $X(\text{In})=80\%$  have same  $P$  within  $\sim 4\%$ . Clearly, the linear polarization ratio  $P$  solely cannot be used to indicate geometrical anisotropy or composition.

### D. Critical QD size for the variation in FSS( $\sigma$ ) to fall below a given threshold

For the fixed number of atoms in the dot  $N_1^{(\text{dot})}$ , FSS( $\sigma$ ) obeys certain probability distribution with the mean value and variance  $(\mu, \text{Var})=(\mu_1, \text{Var}_1)$ . With the increase in the dot size to  $N_2^{(\text{dot})} > N_1^{(\text{dot})}$ , FSS( $\sigma$ ) follows the probability distribution with  $(\mu_2, \text{Var}_2)$ . However, for the fixed  $N_{\text{atoms}}$ , the sampling distribution of the  $\mu$  becomes approximately normal regardless of the distribution of the original variable, and  $\text{Var} \rightarrow \text{Var}_{\text{fin}} = \text{Var}/N_{\text{atoms}}$  (Central Limit Theorem).<sup>26</sup> Thus, for  $N_1^{(\text{dot})}$ ,  $\text{Var}_{\text{fin}_1} = \text{Var}/N_1^{(\text{dot})}$  and for  $N_2^{(\text{dot})}$ ,  $\text{Var}_{\text{fin}_2} = \text{Var}/N_2^{(\text{dot})}$ . This enables us to establish relationship between the variance's of different  $N_{\text{atoms}}$ :  $N_1^{(\text{dot})} \text{Var}_{\text{fin}_1} \sim N_2^{(\text{dot})} \text{Var}_{\text{fin}_2}$ . Hence, one can estimate the number of at-

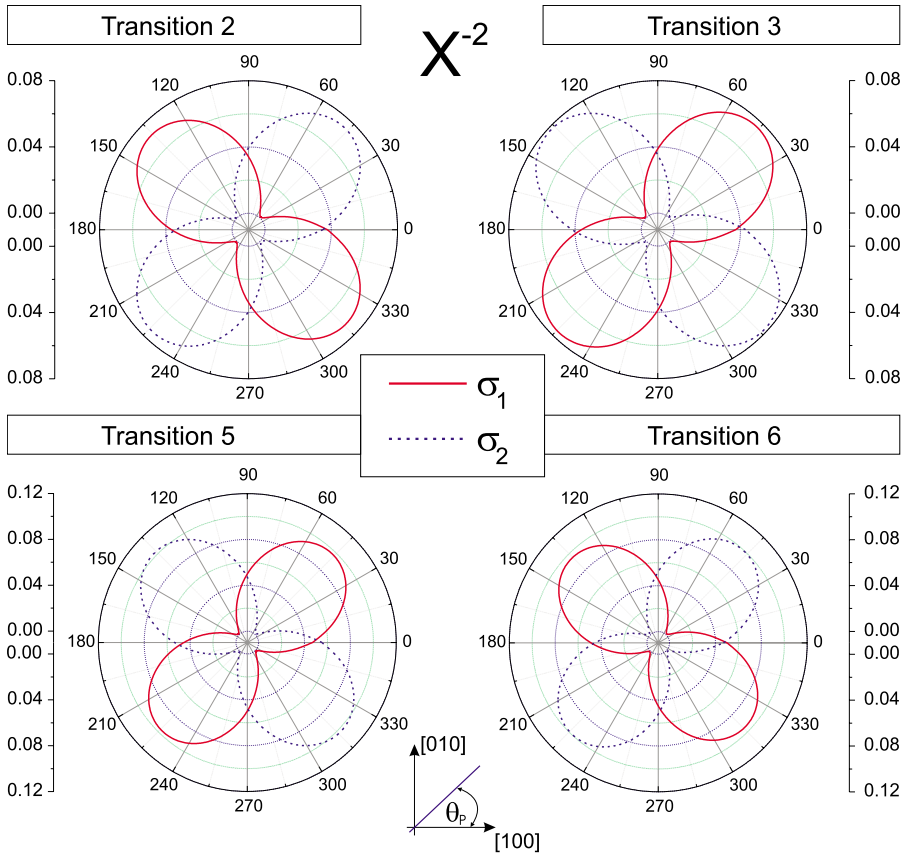


FIG. 4. (Color online) Polarization directions of four optically active transitions of  $X^{-2}$  as they vary with  $\sigma$ . Polarization directions of transition 4 are not shown as they are overlapping for  $\sigma_1$  and  $\sigma_2$  (see Table I).

oms in the dot so that the variance falls below a given threshold. For example, our model dot contains  $N_1^{(\text{dot})} \approx 28\,993$  atoms (of which 1/2 are on cation sublattice, within which 60% are In atoms), and  $\text{Var}_1 = 6.52 (\mu\text{eV})^2$ . To get variance  $\text{Var}_2$  that is 20% of the  $\text{Var}_1$ , a dot has to contain  $N_2^{(\text{dot})} \geq 181\,000$  atoms. This can be, e.g., quantum box with size  $25 \times 25 \times 7$  (in nanometers), or half-sphere with diameter 25 nm, in which case height of such dot is by a factor of 6 larger than height of our model dot. We tested the validity of our simple formula by performing many-body pseudopotential calculations for different  $N_{\text{atoms}}$  and found that it gave a good estimate for the required number of atoms in the dot to get a targeted variance.

#### IV. POLARIZATION DIRECTIONS FOR MULTIEXCITONIC TRANSITIONS

We next move from monoexciton (one hole  $N_h=1$ ; one electron  $N_e=1$ ) to multiexcitonic (ME) transitions  $(N_h, N_e) \rightarrow (N_h-1, N_e-1)$ . Here  $(N_h, N_e) = (1, 3)$  is denoted as  $X^{-2}$ ;  $(2, 2)$  is denoted as  $XX^0$ ;  $(3, 2)$  is denoted as  $XX^{+1}$ , and  $(2, 3)$  is denoted as  $XX^{-1}$ . Figure 3 shows schematically the calculated initial and final single-particle (SP) levels and the initial and final many-particle levels for the emission from  $XX^{-1}$  [Fig. 3(a)] and  $XX^{+1}$  [Fig. 3(b)] multiexcitons. While  $X^{-2}$  (not shown) has five optically active transitions and one dark,<sup>27</sup>  $XX^0$  (not shown) has two optically active and one dark ( $XX^0$  does not have fine structure, and two optically active transitions originate from FSS of the final state  $X^0$ , see, e.g., Ref. 10). Emission from  $XX^{+1}$ ,  $XX^{-1}$  multiexcitons

each have three optically active transitions and one dark, as shown in Fig. 3. For both emissions, from  $XX^{+1}$  and  $XX^{-1}$  multiexcitons, FSS originate from the final states (the initial state is double degenerate in both cases) and transitions 1–3 are optically active whereas the transition 4 is dark. As in the case of polarization directions of monoexciton transitions, we find that ME transitions also show strong dependence on atomic-scale alloy randomness, as illustrated in Table I, giving the polarization angle  $\theta_p$  for different random realizations  $\sigma_i$ .

We find that it is not possible to establish deterministic relationship between polarization directions of given ME transitions in dots that differ in RRs. Even for the fixed QD geometry and stoichiometry, RRs determine the polarization directions of the excitonic transitions. These results suggest that the experimental findings of Poem *et al.*<sup>6</sup> that different ME transitions have well defined polarization directions cannot be of general validity. Furthermore, the effect of RRs sheds light on a recent conflicting experimental results on the polarization state of  $X^{-2}$  measured on QDs produced by the same growth protocol, and both emitting  $\sim 1.3$  eV. Ediger *et al.*<sup>27</sup> found the polarization directions of the optically active transitions of  $X^{-2}$  to be oriented along  $[110]$  and  $[1\bar{1}0]$  directions, whereas Poem *et al.*<sup>6</sup> reported  $[120]$  and  $[2\bar{1}0]$  polarization directions. Who is right? We suggest that the differences between these two experimental reports on the polarization states of  $X^{-2}$  originate from the random realizations of  $\text{Ga}_{1-x}\text{In}_x\text{As}$  QDs. Figure 4 shows two distinct cases where, for the fixed QD geometry and composition, the polarization directions of four optically active transitions of  $X^{-2}$

swap polarization directions with RRs. For example, transition 2 is oriented along  $[110]$  for  $RR=\sigma_1$ , but for  $RR=\sigma_2$  along  $[\bar{1}\bar{1}0]$ .

## V. SUMMARY

We have provided clear evidence for the effects of atomic-scale randomness on the optical properties of alloyed  $\text{Ga}_{1-x}\text{In}_x\text{As}$  QDs. We find that random realizations determine monoexciton's FSS, varying more than a factor of 7 with  $\sigma$ , and the sign and magnitude of the linear polarization ratio. The polarization directions of multiexcitonic transitions also strongly depend on atomic-scale alloy randomness, so different multiexciton emission lines do not have fixed polarization directions. Our findings imply that even if one is able to produce two alloyed QDs of the same size, shape, and composition profile, these two dots may not have identical spectra.

*Note added in proof.* Recent correspondence with Sheng and Xu, for which we are grateful, has indicated that in Ref. 15 they have apparently investigated the effect of *intermixing profile*, not the effect of atom-by-atom random substitution, on the optical polarization. Hence, they have examined a different problem than we have. Specifically, they have used in Ref. 15 a theoretical method that does not have atomic

resolution (the effective bond-orbital method), and considered two cases: (i) a uniform distribution of Ga and In in (In, Ga) As dots, for which they find in their calculation a single polarization  $P$ . For the same case of macroscopically uniform composition, but allowing each cation lattice site to be occupied randomly by either Ga or In (consistent with the composition), we find in this paper different polarizations, with a range described in Fig. 2(a). We thus determined that different RR profoundly affect the polarization. Thus, our result is very different than the result of Sheng and Xu. They have further considered (ii) a nonuniform distribution characterized by an “intermixing profile” selected randomly. In this case, Sheng and Xu find different polarizations for differently selected *composition profiles*. However, they have concluded that “random intermixing effects . . . does not affect much the optical anisotropy.”<sup>15</sup> They further conclude that “the polarization property is shown to be insensitive to the random intermixing effect which makes it an appropriate tool for characterizing structure of quantum dots.”<sup>15</sup> We have not studied nonuniform composition profiles.

## ACKNOWLEDGMENTS

This work was funded by the U. S. Department of Energy, Office of Science, under NREL Contract No. DE-AC36-08GO28308.

\*Corresponding author. alex\_zunger@nrel.gov

<sup>1</sup>T. Muto and Y. Takagi, *The Theory of Order-Disorder Transitions in Alloys* (Academic, New York, 1956).

<sup>2</sup>J. C. Woolley, in *Compound Semiconductors*, edited by R. K. Willardson and H. L. Goering (Reinhold, New York, 1962), p. 3.

<sup>3</sup>S.-H. Wei and A. Zunger, *Appl. Phys. Lett.* **56**, 662 (1990).

<sup>4</sup>M. Ediger, G. Bester, A. Badolato, P. M. Petroff, K. Karrai, A. Zunger, and R. J. Warburton, *Nat. Phys.* **3**, 774 (2007).

<sup>5</sup>B. Urbaszek, R. J. Warburton, K. Karrai, B. D. Gerardot, P. M. Petroff, and J. M. Garcia, *Phys. Rev. Lett.* **90**, 247403 (2003).

<sup>6</sup>E. Poem, J. Shemesh, I. Marderfeld, D. Galushko, N. Akopian, D. Gershoni, B. D. Gerardot, A. Badolato, and P. M. Petroff, *Phys. Rev. B* **76**, 235304 (2007).

<sup>7</sup>P. A. Dalgarno, J. M. Smith, J. McFarlane, B. D. Gerardot, K. Karrai, A. Badolato, P. M. Petroff, and R. J. Warburton, *Phys. Rev. B* **77**, 245311 (2008).

<sup>8</sup>M. S. Skolnick and D. J. Mowbray, *Annu. Rev. Mater. Res.* **34**, 181 (2004).

<sup>9</sup>G. Bester, S. Nair, and A. Zunger, *Phys. Rev. B* **67**, 161306(R) (2003).

<sup>10</sup>R. Seguin, A. Schliwa, S. Rodt, K. Pötschke, U. W. Pohl, and D. Bimberg, *Phys. Rev. Lett.* **95**, 257402 (2005).

<sup>11</sup>See, e.g., M. Pelton, C. Santori, J. Vuckovic, B. Zhang, G. S. Solomon, J. Plant, and Y. Yamamoto, *Phys. Rev. Lett.* **89**, 233602 (2002).

<sup>12</sup>I. Favero, G. Cassaboïs, A. Jankovic, R. Ferreira, D. Darson, C. Voisin, A. Badolato, P. M. Petroff, and J. M. Gérard, *Appl. Phys. Lett.* **86**, 041904 (2005).

<sup>13</sup>I. Favero, G. Cassaboïs, D. Darson, C. Voisin, C. Delalande, Ph. Roussignol, and J. M. Gérard, *Physica E (Amsterdam)* **26**, 51

(2005).

<sup>14</sup>S. Seidl, B. D. Gerardot, P. A. Dalgarno, K. Kowalik, A. W. Holleitner, P. M. Petroff, K. Karrai, and R. J. Warburton, *Physica E (Amsterdam)* **40**, 2153 (2008).

<sup>15</sup>W. Sheng and S. J. Xu, *Phys. Rev. B* **77**, 113305 (2008).

<sup>16</sup>V. Preisler, T. Grange, R. Ferreira, L. A. de Vaulchier, Y. Guldner, F. J. Teran, M. Potemski, and A. Lemaître, *Phys. Rev. B* **73**, 075320 (2006).

<sup>17</sup>S. Hameau, J. N. Isaia, Y. Guldner, E. Deleporte, O. Verzellen, R. Ferreira, G. Bastard, J. Zeman, and J. M. Gérard, *Phys. Rev. B* **65**, 085316 (2002).

<sup>18</sup>P. N. Keating, *Phys. Rev.* **145**, 637 (1966).

<sup>19</sup>L.-W. Wang and A. Zunger, *Phys. Rev. B* **59**, 15806 (1999).

<sup>20</sup>A. Franceschetti, H. Fu, L.-W. Wang, and A. Zunger, *Phys. Rev. B* **60**, 1819 (1999).

<sup>21</sup>G. A. Narvaez, G. Bester, and A. Zunger, *Phys. Rev. B* **72**, 245318 (2005).

<sup>22</sup>M. Grundmann, O. Stier, and D. Bimberg, *Phys. Rev. B* **52**, 11969 (1995).

<sup>23</sup>G. Bester and A. Zunger, *Phys. Rev. B* **72**, 165334 (2005).

<sup>24</sup>G. Bester, X. Wu, D. Vanderbilt, and A. Zunger, *Phys. Rev. Lett.* **96**, 187602 (2006).

<sup>25</sup>G. Bester, A. Zunger, X. Wu, and D. Vanderbilt, *Phys. Rev. B* **74**, 081305(R) (2006).

<sup>26</sup>J. F. C. Kingman, G. E. H. Reuter, and N. J. Hitchin, *Probability, Statistics and Analysis* (Cambridge University Press, UK, 2008).

<sup>27</sup>M. Ediger, G. Bester, B. D. Gerardot, A. Badolato, P. M. Petroff, K. Karrai, A. Zunger, and R. J. Warburton, *Phys. Rev. Lett.* **98**, 036808 (2007).